

Tunable Optical Nanocavity Based on Modulation of Near-Field Coupling Between Subwavelength Periodic Nanostructures

Wataru Nakagawa and Yeshaiah Fainman, *Fellow, IEEE*

Abstract—We present the design and analysis of a tunable resonant optical filter based on modulation of the near-field coupling between two subwavelength periodic nanostructures embedded in a Fabry–Pérot cavity. Due to the transverse localization of the optical field in the subwavelength gratings, their relative positioning strongly influences the near-field coupling between them and, thus, affects the resonance of the cavity. Rigorous electromagnetic analysis tools are applied to determine the optical characteristics of the filter with respect to the nanostructure lateral alignment, small variations in the shape of the nanostructures, and the physical separation of the nanostructures.

Index Terms—Nanotechnology, optical filters, optical MEMS, optical nanostructures, optical near-field coupling, optical near-field localization, optical propagation in nonhomogeneous media, optical resonators.

I. INTRODUCTION

RECENT innovations in nanoscale optical technologies have enabled a significant number of developments in various optical and photonic application areas. One specific area of investigation is near-field optical coupling in optical nanostructures, encompassing, for example, developments such as near-field optical microscopy [1]–[5], photonic integrated circuits [6], artificial dielectric materials [7], as well as photonic crystal nanocavities [8]–[10] and resonant filters [11], [12]. In previous work [13], [14], we described the polarization-dependent transverse localization of the optical field inside a subwavelength periodic nanostructure and studied its application to the enhancement of nonlinear optical phenomena. In this paper, we investigate a novel tunable resonant optical cavity design based on the proximity-dependent near-field coupling between a pair of transverse field localization nanostructures and characterize its performance characteristics using rigorous electromagnetic analysis techniques.

The filter is composed of two planar dielectric mirrors forming a Fabry–Pérot cavity, with a field localization nanostructure affixed to the inner surface of each mirror. Due to the strong transverse localization of the optical field in the

nanostructures, relative displacement of one side of the cavity (mirror and nanostructure) with respect to the other in the transverse—as well as the longitudinal—direction results in a modification of the near-field optical coupling between the nanostructures. As the nanostructures are embedded in the cavity, this perturbation of the physical layout of the structure alters the effective optical path length inside the Fabry–Pérot cavity and, consequently, results in a modulation of the overall transmission resonance properties of the filter. Thus, dramatic changes in the external optical properties of the cavity result from extremely small physical movement of the nanostructures embedded in the cavity due to the high sensitivity of the near-field optical coupling between the nanostructures.

This device can be used to construct a tunable filter or modulator with a wide range of potential applications including telecommunications, optical information processing, and optical sensors. In addition, due to the compatibility of the device with standard materials and nanofabrication technologies, a device of this type based on physical displacement of nanostructures has the added advantage of being readily compatible with microelectromechanical systems (MEMS) technology. Along with other investigations into tunable optical filters compatible with optical MEMS, such as two-dimensional photonic crystal-based optical cavities with displacement-sensitive photonic crystal mirrors [15] or a rotating noncircular cavity defect [16], these results suggest that nanostructured photonic devices based on near-field optical phenomena may provide exciting new applications for optical MEMS technologies.

The design and analysis of the tunable optical cavity based on near-field localization nanostructures is presented below, followed by the performance characteristics of the filter with respect to transverse and longitudinal translations. Compensation for fabrication errors through nanostructure alignment is discussed in the concluding section.

II. DESIGN AND ANALYSIS

A schematic diagram of the tunable resonant optical cavity for the transverse electric (TE) polarization (i.e., with the electric field parallel to the grating grooves) is shown in Fig. 1. The cavity consists of two distributed Bragg mirrors, each composed of a number of planar dielectric layers with alternating high and low indices of refraction. A transverse optical field localization nanostructure is affixed to the inner surface of each mirror, and together the pair of nanostructures almost fill the body of the

Manuscript received October 17, 2003; revised February 4, 2004. This work was supported in part by the Defense Advanced Research Projects Agency, in part by the National Science Foundation, in part by the U. S. Air Force Office of Scientific Research, and in part by the Applied Micro Circuits Corporation.

W. Nakagawa is with the Institute of Microtechnology, University of Neuchâtel, Neuchâtel 2000, Switzerland (e-mail: wataru.nakagawa@unine.ch).

Y. Fainman is with the Department of Electrical and Computer Engineering, University of California at San Diego, La Jolla, CA 92093-0407 USA (e-mail: fainman@ece.ucsd.edu).

Digital Object Identifier 10.1109/JSTQE.2004.828489

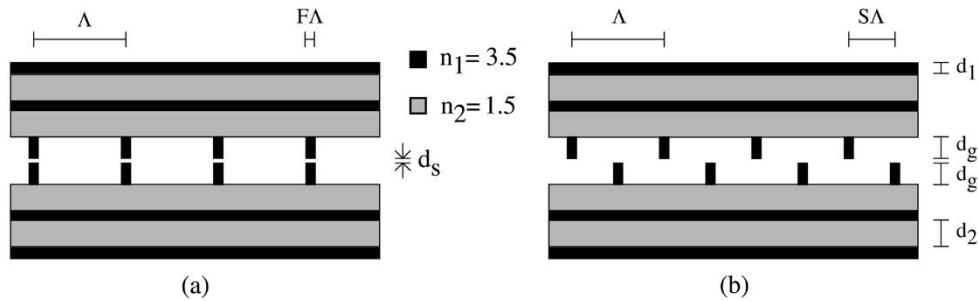


Fig. 1. Schematic diagram of the TE polarization tunable cavity nanostructure. Each mirror is composed of two pairs of alternating high and low refractive index layers having thicknesses $d_1 = 0.0714\lambda_0$ and $d_2 = 0.1667\lambda_0$, respectively. Each nanostructure is an infinite periodic square grating with period $\Lambda = 0.6\lambda_0$, $F = 0.1$, and $d_g = 0.1343\lambda_0$. The separation between the nanostructures is taken to be $d_s = 0.01\lambda_0$. Two cases are shown. (a) Two nanostructures aligned, with $S = 0.0$. (b) Nanostructures at maximum separation with $S = 0.5$.

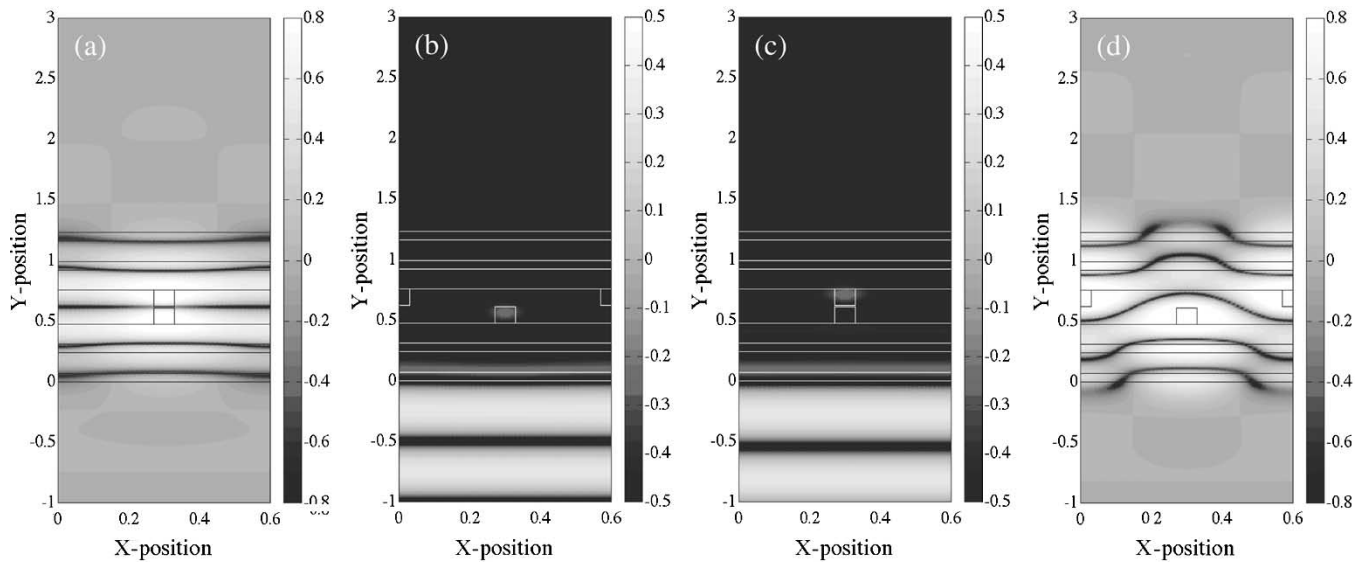


Fig. 2. Normalized magnitude (logarithmic scale) of the optical field inside one period of the TE polarization tunable cavity nanostructure. At the design wavelength $\lambda = \lambda_0$: (a) in the transmissive configuration with $S = 0.0$; (b) in the reflective configuration with $S = 0.5$. At an offset wavelength $\lambda = 1.0802\lambda_0$ with: (c) $S = 0.0$ and (d) $S = 0.5$ (the resonance condition for this wavelength).

cavity. Each nanostructure consists of a transverse infinite sub-wavelength periodic grating with period $\Lambda = 0.6\lambda_0$, fill factor $F = 0.10$, and thickness $d_g = 0.1343\lambda_0$, where λ_0 is the intended resonant optical wavelength (all spatial dimensions are scaled to this parameter). The two nanostructures are separated by a small air gap $d_s = 0.01\lambda_0$. Due to the strong transverse near-field localization in the subwavelength gratings, the relative lateral position of the two gratings—defined by parameter S [see Fig. 1(b)]—influences the optical coupling between them. Only values of S between $S = 0$ and $S = 0.5$ are considered, as the symmetry of the infinitely periodic structure renders all values of S to be equivalent to values in the range 0.0–0.5. The two extreme cases are shown: Fig. 1(a) corresponds to the case when the two gratings are aligned (shift parameter $S = 0.0$), and Fig. 1(b) corresponds to the case with the two gratings offset by half a period (shift parameter $S = 0.5$). The change in the relative position of the two gratings modifies the near-field optical coupling between them, changing the effective optical path length inside the cavity, thus altering the resonance of the cavity as a whole.

As an electromagnetic modeling tool, we apply the rigorous coupled-wave analysis (RCWA) method [17]–[19], which is

based on a Fourier modal decomposition of the fields inside a transversely periodic structure and is a well-established technique for analyzing subwavelength periodic gratings. Using this method, we investigate the optical performance characteristics of the tunable cavity shown in Fig. 1. For the results presented in this paper, we set $n_1 = 3.5$ and $n_2 = 1.5$, approximately corresponding to the indices of refraction of GaAs and oxidized AlAs, respectively, at an operating wavelength of $\lambda_0 = 1.55 \mu\text{m}$. The planar layers of the device form standard quarter-wave dielectric mirrors with layer thicknesses $d_1 = 0.0714\lambda_0$ and $d_2 = 0.1667\lambda_0$ for the given values of the refractive index. The normalized field magnitude at the design wavelength ($\lambda = \lambda_0$) inside and immediately surrounding one period of the structure for the cases $S = 0.0$ and $S = 0.5$ are shown in Fig. 2(a) and (b), respectively. In Fig. 2(a), the incident wavelength is resonant with the cavity, and the field is transmitted through the structure. In Fig. 2(b), the resonance of the cavity is altered due to the relative shift of the nanostructured gratings, and the incident field is reflected, as demonstrated by the standing wave pattern in front of the structure. In both figures, the transverse localization of the field in the narrow high refractive index region of the

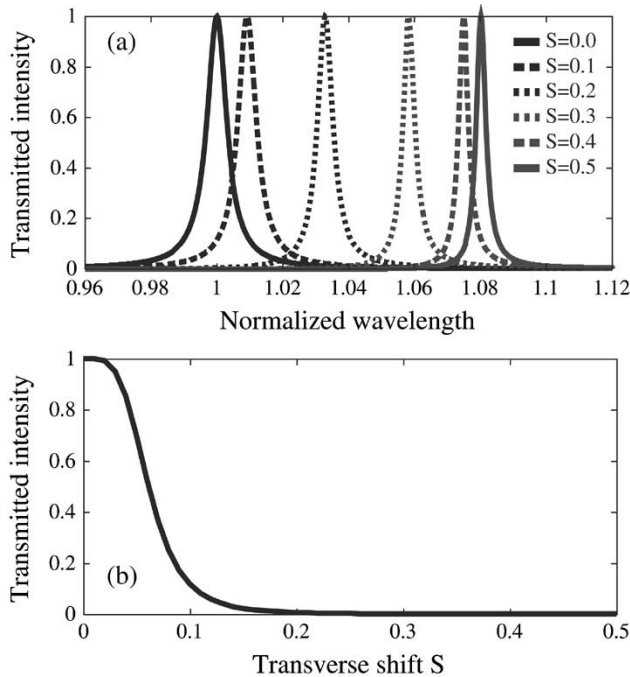


Fig. 3. Transmitted intensity for the TE polarization tunable cavity: (a) versus wavelength (λ/λ_0) for several values of the translation parameter S and (b) versus translation parameter S for the design wavelength $\lambda = \lambda_0$.

subwavelength gratings can be clearly seen. In addition, due to the subwavelength period of the structure, the transmitted and reflected fields in the far field do not exhibit any transverse modulation because of the interaction with the nanostructure. Similar results at an offset wavelength ($\lambda = 1.0802\lambda_0$) are presented in Fig. 2(c) and (d), for the $S = 0.0$ and $S = 0.5$ cases, respectively. At this wavelength, the device transmits for the $S = 0.5$ case and reflects for the $S = 0.0$ case, although in both cases the transverse localization of the field due to the nanostructures embedded in the cavity can still be observed.

III. TUNABILITY BY LATERAL DISPLACEMENT

Next, we investigate the optical performance of the tunable cavity by examining the transmissivity of the cavity. Fig. 3(a) shows the transmitted intensity as a function of wavelength for several lateral shift positions of the nanostructures (indicated by the coefficient S). Fig. 3(a) shows that the resonance of the cavity can be controlled over a certain range (in this example, approximately 0.08 in units of normalized wavelength) by varying the relative translational shift S of the nanostructures from $S = 0$ to $S = 0.5$. In general, the quality factor (Q) of the cavity is chosen to meet the needs of the target application; in this case, the number of Bragg mirror layers is chosen such that the device is approximately fully transmissive ($>99.98\%$) for $S = 0.0$, and approximately fully reflective ($<0.001\%$) for $S = 0.5$ at a certain wavelength. Fig. 3(b) shows the transmitted intensity as a function of the lateral shift S at the design wavelength and illustrates the functionality of the device as an intensity modulator. In principle, it is also possible to use this device to achieve variable transmissivity by controlling the nanostructure shift over the range between the on-off states, although this

application would require correspondingly higher positioning accuracy.

As is expected for a Fabry–Pérot cavity, the resonance of the tunable cavity can also be adjusted by modulating the size of the central layer of the cavity. Fig. 4(a) shows the transmission peaks for several structures similar to that of Fig. 1 with $S = 0.0$ and differing nanostructure heights d_g but constant nanostructure separation d_s . In this comparison, the effective optical length of the cavity (i.e., the distance between the mirrors) is varied, but the near-field optical coupling between the nanostructures is held constant. The resonance wavelength varies linearly as the depth of the subwavelength grating and, consequently, the length of the cavity, is altered.

In addition to the height of the nanostructures, the width of the periodic nanostructures will also influence the transmission characteristics of the device. The influence of the nanostructure fill factor (F) on the transmitted wavelength is shown in Fig. 4(b) and (c) for the $S = 0.0$ and $S = 0.5$ cases, respectively. In each case, a slight variation in the nanostructure fill factor from the design value results in a corresponding shift in the resonance wavelength.

IV. TUNABILITY BY LONGITUDINAL DISPLACEMENT

The effect of the size of the separation (d_s) between the two nanostructures on the resonance wavelength is presented in Fig. 5(a), which shows the increase in the resonance wavelength as the nanostructure separation d_s is increased for the $S = 0.0$ case. As in Fig. 4(a), as the length of the cavity increases, we expect the resonance wavelength to increase. However, unlike in Fig. 4(a), where the height of the nanostructures is increased but the separation between them is kept constant, as the space between the nanostructures is increased, in addition to increasing the physical length of the cavity, the near-field optical coupling between the nanostructures is also affected. Thus, we expect there to be a nonlinear relationship between the nanostructure separation d_s and the resonance wavelength of the cavity (at least for small values of d_s where near-field optical phenomena are still significant). Fig. 5(b) shows results similar to Fig. 5(a), but for the $S = 0.5$ case, and Fig. 5(c) shows the resonance wavelength versus nanostructure gap d_s for the $S = 0.0$, $S = 0.25$, and $S = 0.5$ cases. From Fig. 5(c), it is clear that the difference in the resonance wavelength between the $S = 0.0$ and $S = 0.5$ cases is greatest for the smallest value of d_s and that this difference decreases as the nanostructure separation d_s increases. In addition, the slopes of the curves corresponding to the resonance wavelengths of the three cases are nonlinear, at least for small values of d_s (e.g., less than 0.15). As suggested above, this behavior results from the dependence of the near-field optical coupling between the nanostructures on their separation, in both the transverse and longitudinal directions.

However, this description is not sufficient to fully explain the results shown in Fig. 5(c). Note that while the resonance wavelength is essentially identical for the $S = 0.0$, $S = 0.25$, and $S = 0.5$ cases for values of d_s greater than approximately 0.15, the resonance wavelength is also close to constant. While we expect the resonance wavelengths in the three cases to converge as

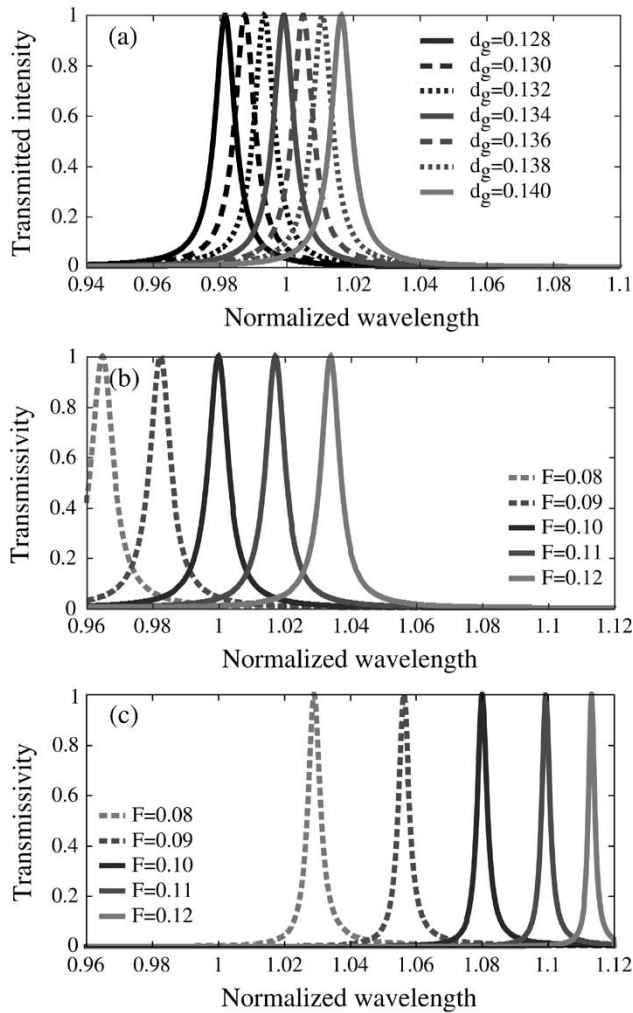


Fig. 4. Transmitted intensity of the TE polarization tunable cavity versus normalized wavelength for: (a) several nanostructure layer depths d_g with $S = 0.0$; (b) several nanostructure fill factors F with $S = 0.0$; and (c) several values of F with $S = 0.5$.

the nanostructure separation is increased, the resonance wavelength should also continue to increase as the physical length of the cavity is increased. The results in Fig. 5(c) arise from a second resonance present in the system, of the nanostructure and Bragg mirror, rather than the cavity. Fig. 6(a) shows the reflectivity of the four planar layers of one Bragg mirror, approximately constant over the wavelength range of interest, as intended. However, as shown in Fig. 6(b), for the mirror plus one set of nanostructures (i.e., one side of the cavity), there are clear resonance features in the reflectivity spectrum. This resonance arises from the structure of each half of the cavity, and does not depend on the relative alignment or separation of the nanostructures to form the full cavity, although this resonance will affect the performance of the entire device. Specifically, the position of the resonance feature observed in the center of Fig. 6(b), approximately 1.15 in units of normalized wavelength, corresponds to the asymptotic value of the resonance wavelength observed in Fig. 5(c).

In order to separate these two phenomena, we consider a modified structure like that of Fig. 1, but with the thicknesses of the planar layers (d_1 and d_2) increased by 10%. The reflectivity

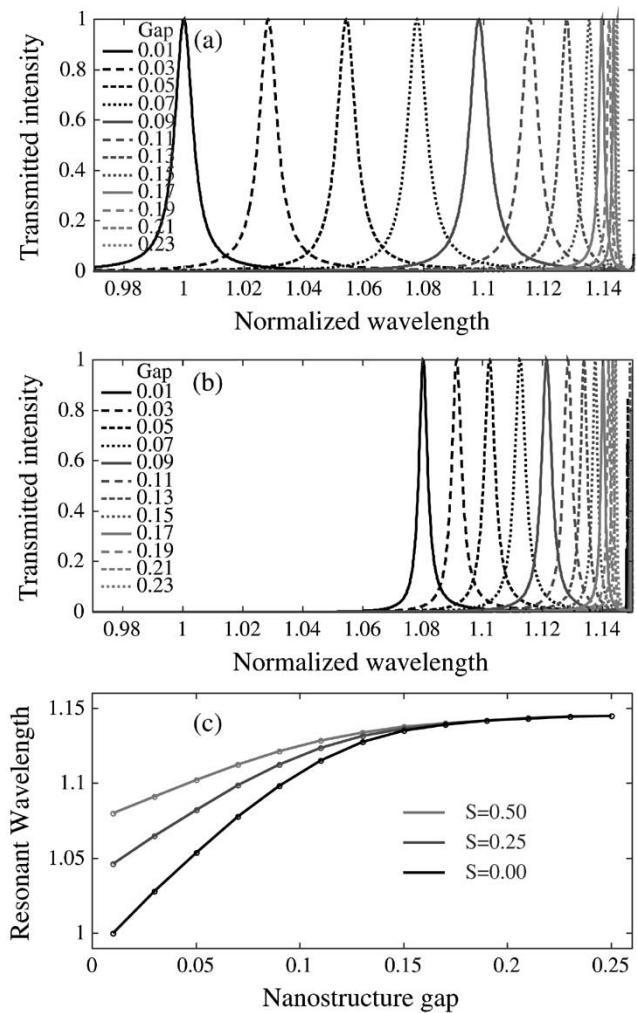


Fig. 5. Transmitted intensity of the TE polarization tunable cavity versus normalized wavelength for several values of the nanostructure separation d_s with: (a) shift parameter $S = 0.0$; (b) shift parameter $S = 0.5$; and (c) the resonance wavelength versus nanostructure separation d_s for the $S = 0.0$, $S = 0.25$ and $S = 0.5$ cases.

spectrum of one side of this modified cavity (four planar layers plus one nanostructure layer) is presented in Fig. 6(c) and shows that although the resonance is still present, it has been shifted to a longer wavelength. The performance of the total modified device is presented in Fig. 7, which shows the resonance wavelength versus nanostructure separation d_s for the $S = 0.0$ and $S = 0.5$ cases. In these results the two phenomena—the near-field optical coupling between the nanostructures and the resonance of the half cavity—have been separated in wavelength and can, thus, be distinguished. For nanostructure gaps above approximately 0.2 in units of normalized wavelength, the rolloff in the resonance wavelength reflects the influence of the reflection resonance present in the mirror plus nanostructure sub-element, as in the previous results. However, for nanostructure gaps ranging from 0 to approximately 0.2, the gradually diminishing effect of the nanostructure alignment S on the resonance wavelength with increasing separation is clearly observed and reflects the weakening near-field optical coupling between the nanostructures. Thus, the resonance characteristics of the optical filter

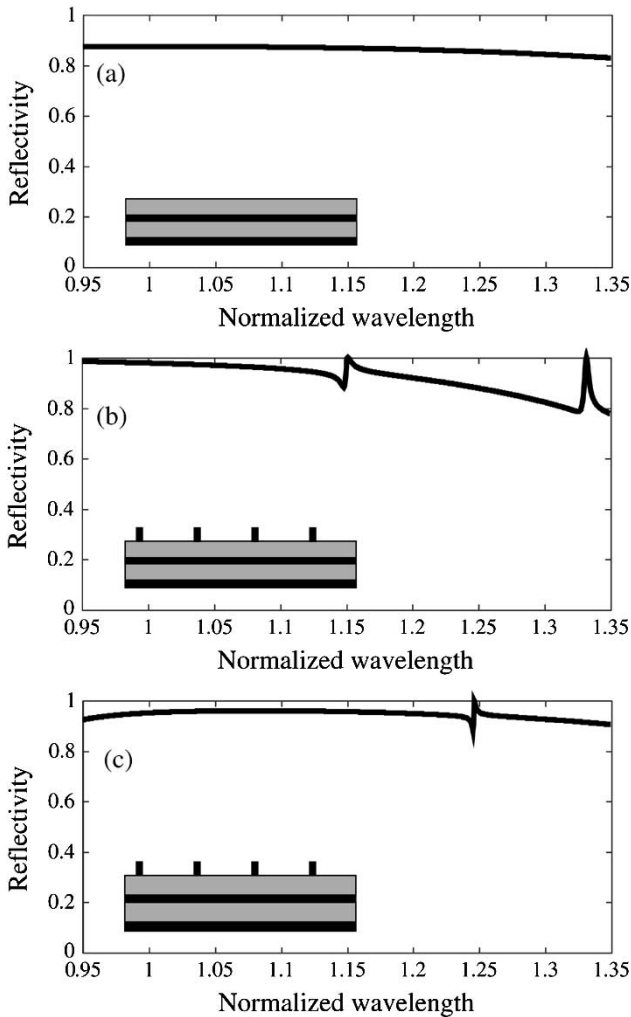


Fig. 6. Mirror reflectivity versus normalized wavelength for: (a) the four-layer Bragg mirror as shown in Fig. 1; (b) the four planar layer mirror with one set of periodic nanostructures (corresponding to half of the cavity structure shown in Fig. 1); and (c) the modified half-cavity structure where the thickness of each planar mirror layer has been increased by 10%.

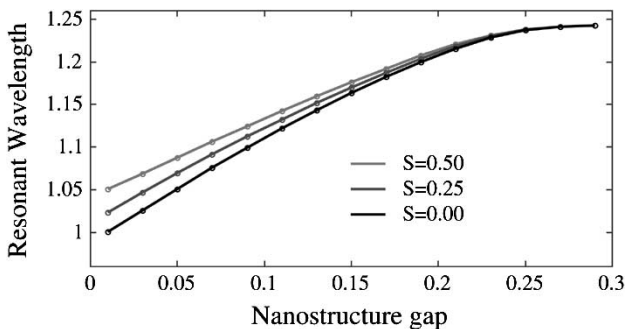


Fig. 7. Resonance wavelength versus nanostructure separation d_s for the modified cavity structure—similar to the structure of Fig. 1 but with the thickness of each planar layer in the Bragg mirrors increased by 10%—for the aligned ($S = 0.0$) and two offset ($S = 0.25$ and $S = 0.5$) cases.

are very sensitive to perturbations of the near-field optical coupling between the nanostructures embedded within the cavity due to both transverse and longitudinal displacement of one nanostructure with respect to the other.

In addition, comparing the resonance wavelengths in $S = 0.0$ and $S = 0.5$ cases for the original filter design [see Fig. 5(c)] and the modified design (see Fig. 7), we find the tunable range of the device to be approximately 0.08 and 0.05, respectively, in units of the design wavelength. This indicates that the tunable range of the device due to transverse shifting of the nanostructures is also dependent on the longitudinal reflectivity characteristics of the cavity mirrors. In a simplistic model, these two effects might be considered to be orthogonal and, therefore, not to have a strong mutual influence. However, these results show that there is in fact a strong relationship between the various cavity parameters and the observed filter characteristics and suggest that due to the strong optical near-field coupling and resonances present in the device, a unified and rigorous electromagnetic analysis of the device is necessary in order to accurately determine the filter properties. Assuming adequate analysis tools exist, however, this complexity provides an important advantage: the implementation of a tunable optical cavity based on near-field coupling between nanostructures with optical MEMS technology permits great flexibility in device performance, as the various parameters of the device—for example, design wavelength, mirror composition, actuation in one or two axes of motion, nanostructure geometry, or fabrication tolerances—can be optimized to best suit the requirements of the particular application of interest.

V. DISCUSSION AND CONCLUSION

A tunable resonant optical filter design based on standard materials and fabrication processes is a potentially useful element for photonic and electronic system integration. The wide tunability of the cavity may provide additional flexibility, for example, to decrease the necessary fabrication tolerances in the fabrication of photonic nanostructure devices or to compensate for variations in the device operating environment (e.g., temperature). Given that a change in either the shift parameter S or the separation of the two nanostructures (d_s) can shift the resonance to a longer wavelength, a certain amount of fabrication tolerance can be included by designing the resonance of the cavity to be at an offset slightly shorter wavelength than desired, and then adjusting one of the above parameters to achieve resonance at the desired wavelength. Although this compensation does come at the expense of reducing the tunable range of the device, it is possible to minimize the wavelength offset based on the expected fabrication tolerances and, thus, maximize the tunable range, allowing the design to be optimized for each specific application. Finally, the ready compatibility of the tunable filter based on near-field optical phenomena in nanostructures with optical MEMS technology provides an important opportunity to expand the range of applications of both technologies, as well as facilitates the evolution of large-scale integrated optical and photonic microsystems.

In summary, we have analyzed the predicted performance of a tunable resonant nanocavity based on the near-field coupling between two periodic nanostructures embedded inside the cavity. Rigorous electromagnetic modeling tools are applied to investigate and visualize the near-field coupling between the nanostructures, as well as to determine the filter

characteristics associated with transverse relative displacement of the nanostructures and changes in the shape of the nanostructures. Finally, a detailed analysis of the influence of the physical separation between the nanostructures on the near-field optical coupling between them and, consequently, the spectral performance of the device is presented. These results demonstrate a new approach to the design of a tunable optical cavity based on the modulation of near-field coupling in a nanostructured optical device and illustrate the potential for a range of novel optical and photonic devices based on near-field optical phenomena in nanostructures.

REFERENCES

- [1] B. Hecht, B. Sick, U. P. Wild, V. Deckert, R. Zenobi, O. J. F. Martin, and D. W. Pohl, "Scanning near-field optical microscopy with aperture probes: Fundamentals and applications," *J. Chem. Phys.*, vol. 112, pp. 7761–7774, May 2000.
- [2] T. Huser, L. Novotny, T. Lacoste, R. Eckert, and H. Heinzelmann, "Observation and analysis of near-field optical diffraction," *J. Opt. Soc. Amer. A, Opt. Image Sci.*, vol. 16, pp. 141–148, Jan. 1999.
- [3] A. Kramer, W. Trapesinger, B. Hecht, and U. P. Wild, "Optical near-field enhancement at a metal tip probed by a single fluorophore," *Appl. Phys. Lett.*, vol. 80, pp. 1652–1654, Mar. 2002.
- [4] E. Flück, M. Hammer, A. M. Otter, J. P. Korterik, L. Kuipers, and N. F. van Hulst, "Amplitude and phase evolution of optical fields inside periodic photonic structures," *J. Lightwave Technol.*, vol. 21, pp. 1384–1393, May 2003.
- [5] L. Vaccaro, L. Aeschimann, U. Staufer, H. P. Herzig, and R. Dändliker, "Propagation of the electromagnetic field in fully coated near-field optical probes," *Appl. Phys. Lett.*, vol. 83, pp. 584–586, July 2003.
- [6] M. Ohtsu, K. Kobayashi, T. Kawazoe, S. Sangu, and T. Yatsui, "Nanophotonics: Design, fabrication and operation of nanometric devices using optical near fields," *IEEE J. Select. Topics Quantum Electron.*, vol. 8, pp. 839–862, July–Aug. 2002.
- [7] F. Xu, R.-C. Tyan, P.-C. Sun, Y. Fainman, C.-C. Cheng, and A. Scherer, "Fabrication, modeling, and characterization of form-birefringent nanostructures," *Opt. Lett.*, vol. 20, pp. 2457–2459, Dec. 1995.
- [8] O. Painter, J. Vuckovic, and A. Scherer, "Defect modes of a two-dimensional photonic crystal in an optically thin dielectric slab," *J. Opt. Soc. Amer. B, Opt. Phys.*, vol. 16, pp. 275–285, Feb. 1999.
- [9] O. Painter, R. K. Lee, A. Scherer, A. Yariv, J. D. O'Brien, P. D. Dapkus, and I. Kim, "Two-dimensional photonic band-gap defect mode laser," *Science*, vol. 284, pp. 1819–1821, June 1999.
- [10] A. A. Erchak, D. J. Ripin, S. Fan, P. Rakich, J. D. Joannopoulos, E. P. Ippen, G. S. Petrich, and L. A. Kolodziejski, "Enhanced coupling to vertical radiation using a twodimensional photonic crystal in a semiconductor light-emitting diode," *Appl. Phys. Lett.*, vol. 78, pp. 563–565, Jan. 2001.
- [11] M. Imada, S. Noda, A. Chutinan, M. Mochizuki, and T. Tanaka, "Channel drop filter using a single defect in a 2-D photonic crystal slab waveguide," *J. Lightwave Technol.*, vol. 20, pp. 873–878, May 2002.
- [12] W. Nakagawa, P.-C. Sun, C.-H. Chen, and Y. Fainman, "Wide-field-of-view narrow-band spectral filters based on photonic crystal nanocavities," *Opt. Lett.*, vol. 27, pp. 191–193, Feb. 2002.
- [13] W. Nakagawa, R.-C. Tyan, P.-C. Sun, and Y. Fainman, "Near-field localization of ultrashort optical pulses in transverse 1-D periodic nanostructures," *Opt. Express*, vol. 7, pp. 123–128, July 2000.
- [14] W. Nakagawa, R.-C. Tyan, and Y. Fainman, "Analysis of enhanced second harmonic generation in periodic nanostructures using modified rigorous coupled-wave analysis in the undepleted pump approximation," *J. Opt. Soc. Amer. A, Opt. Image Sci.*, vol. 19, pp. 1919–1928, Sept. 2002.
- [15] W. Suh, M. F. Yanik, O. Solgaard, and S. Fan, "Displacement-sensitive photonic crystal structures based on guided resonance in photonic crystal slabs," *Appl. Phys. Lett.*, vol. 82, pp. 1999–2001, Mar. 2003.
- [16] K. Takano, T. Sugano, and K. Nakagawa, "Frequency response of rotating shape defect in 2-D photonic crystal for optical tunable filter," in *Proc. 14th Annu. Meeting IEEE Lasers and Electro-Optics Soc.*, 2001, pp. 206–207.
- [17] M. G. Moharam and T. K. Gaylord, "Diffraction analysis of dielectric surface-relief gratings," *J. Opt. Soc. Amer.*, vol. 72, pp. 1385–1392, Oct. 1982.
- [18] N. Chateau and J.-P. Hugonin, "Algorithm for the rigorous coupled-wave analysis of grating diffraction," *J. Opt. Soc. Amer. A, Opt. Image Sci.*, vol. 11, pp. 1321–1331, Apr. 1994.
- [19] L. Li, "Use of Fourier series in the analysis of discontinuous periodic structures," *J. Opt. Soc. Amer. A, Opt. Image Sci.*, vol. 13, pp. 1872–1876, Sept. 1996.

Wataru Nakagawa received the B.S. degree in physics from Stanford University, Stanford, CA, in 1996 and the M.S. and Ph.D. degrees in electrical and computer engineering (applied physics) from the University of California at San Diego, in 1999 and 2002, respectively.

He is currently a Senior Scientist in the Applied Optics group of the Institute of Microtechnology, University of Neuchâtel, Neuchâtel, Switzerland. His research interests encompass near-field optical effects in photonic structures and devices, as well as nonlinear optical phenomena in nanostructures, including the development of rigorous electromagnetic modeling and analysis tools, and the design and characterization of novel photonic nanostructures.

Dr. Nakagawa is a member of the Optical Society of America and the IEEE Lasers and Electro-Optics Society.

Yehiaiahu Fainman (M'93–SM'01–F'03) received the Ph.D. degree from Technion–Israel Institute of Technology in 1983.

He is a Professor of Electrical and Computer Engineering at the University of California at San Diego, La Jolla. He has contributed over 100 manuscripts in referred journals and over 200 conference presentations and conference proceedings. From 1993 to 2001, he was a Topical Editor of the *Journal of the Optical Society of America A, Optical Signal Processing and Imaging Science*. His current research interests are in ultrafast information processing with optical nonlinearities and use of femtosecond laser pulses, near field phenomena in optical nanostructures and nanophotonic devices, quantum communication, multidimensional quantitative imaging, and programmable and multifunctional diffractive and nonlinear optics.

Dr. Fainman is a Fellow of the Optical Society of America. He received the Miriam and Aharon Gutvirt Prize. He has served on several conference program committees and has organized symposia and workshops.